

Inter-Valley Charge Transfer in Short-Wavelength InGaAs-AlAs Quantum-Cascade Lasers

Mykhaylo P. Semtsiv, Martin Wienold, Ismail Bayrakli,
Sebastian Dressler, and W. Ted Masselink

Abstract—We discuss the engineering of the upper-laser-state lifetime in strain-compensated InGaAs-AlAs/InP quantum-cascade lasers emitting at wavelengths between 3 μm and 5 μm . In these short-wavelength designs the energy of the upper laser state is very close to the band edges of the indirect X and L valleys, which opens an additional channel for non-radiative depopulation of the upper laser level. Population inversion between the upper and the lower laser states crucially depends on the dipole matrix element for intersubband transitions between the upper laser state and the lower laser state as well as on the probability of the inter-valley carrier transfer. The inter-valley transfer, made evident through an abrupt increase of threshold current occurs at elevated temperatures because it requires a large-momentum phonon. At low temperatures, the threshold current density is not very dependent on emission wavelength because the phonon population is low and inter-valley scattering not very significant. The overall laser performance, however, degrades as the short wavelength limit is approached.

Index Terms—Intersubband transitions, midinfrared, quantum-cascade laser (QCL), strain-compensated.

DEVELOPMENT of quantum-cascade lasers (QCLs) operating in the 3–5 μm spectral region is driven by a number of applications including gas sensing for both environmental and medical uses, communication, and military countermeasures.

Currently strain-compensated InGaAs-InAlAs/InP QCLs are the lasers of choice for the 3.5–5 μm range due to their low thresholds and high efficiency [1]. Below $\sim 3.3\mu\text{m}$, the interband cascade lasers are more efficient [2]. In intermediate region at the vicinity of 3 μm emission wavelength InAs-AlSb QCLs are favoured [3], since the InP-based QCLs reduce they performance close to 3 μm . In this talk we focus on the constraints on the quantum efficiency of InGaAs-AlAs/InP QCLs as the emission wavelength approaches 3 μm . We also discuss the trade-off between “diagonal” and “vertical” intersubband laser transitions in various active region designs.

Figure 1 pictures a typical short-wavelength InGaAs-AlAs/InP QCL active region design under operation bias. As was shown through the bias-dependent spectral shift of

electroluminescence [4] as well as by the shift of the laser spectrum in a magnetic field [5], the laser transition is composed from several intersubband transitions, especially, 3-1 and 2-1, with the highest dipole matrix elements. Generally, a thicker injection barrier favours the 3-1 transition, while a thinner injection barrier favours the 2-1 transition [5]. The choice of either a “diagonal”, 3-1-like, or a “vertical”, 2-1-like, intersubband transition is critical because they have different degrees of spatial overlap with X- and L-valley states. At the short-wavelength limit, the depopulation of the upper laser state in the indirect valley is the main factor limiting high-temperature laser performance. Hence, by engineering a “more diagonal” intersubband laser transition one could boost the high-temperature laser performance while keeping the upper laser state close to the edge of indirect valleys (i.e. maintaining a very short transition wavelength). On the other hand, for somewhat longer wavelength designs, this inter-valley scattering is of lesser importance due to larger energy difference between the upper laser state and the edge of indirect valleys. In this case the “more vertical” intersubband laser transition is preferable, since it provides higher gain.

Several QCL active region designs, based on the above considerations, with different injection barriers and different doping were designed, grown, processed, and compared [4]–[8]. Figure 2 highlights the emission wavelengths of several QCL designs between 3 μm and 4 μm . The shorter the wavelength, the “more diagonal” intersubband transition was engineered to provide the population inversion. Few test-designs with “vertical” intersubband laser transitions did not lase at the shortest wavelengths, while these with “more diagonal” design did lase up to the temperatures as indicated on Fig. 3.

It is generally accepted that in “diagonal”-transition QCL active region designs gain spectrum broadens compared to “vertical”-transition designs due to higher spatial overlap of the intersubband laser transition with the interface roughness. However, our measurements of the subthreshold electroluminescence half-widths for various QCL designs (see Fig. 3) do not support this view. Hence, we relate the QCL performance degradation at shorter wavelengths to be exclusively related to the inter-valley charge transfer. This interpretation is also supported by a biexponential thermal dependence of the threshold current density, observed only in QCLs operating at wavelengths as short as 3.3 μm and 3.05 μm

(see Fig. 4). We consider the rapid increase of the threshold current density beyond 150 K on Fig. 4 to represent the onset of the thermally activated inter-valley charge transfer. This threshold current behaviour was not observed in QCLs operating at somewhat longer wavelength ($>3.6\mu\text{m}$), where the upper laser state is sufficiently energetically separated from the indirect valleys edge.

To summarize, the high-temperature operation of very-short-wavelength QCLs is found to be limited by depopulation of the upper laser state into the indirect valleys when the upper laser state approaches the edge of indirect valleys in conduction band. Thus, further progress in the InP-based QCL active region engineering might be directed towards effective exploitation of the Γ -to-X/L valley spacing.

REFERENCES

- [1] J. S. Yu, A. Evans, S. Slivken, S. R. Darvish, and M. Razeghi, "Temperature dependent characteristics of $\lambda \sim 3.8 \mu\text{m}$ room-temperature continuous-wave quantum-cascade lasers," *Appl. Phys. Lett.*, vol. 88, p. 251118, June 2006.
- [2] R. Q. Yang, C. J. Hill, and B. Yang, "High-temperature and low-threshold midinfrared interband cascade lasers," *Appl. Phys. Lett.*, vol. 87, p. 151109, Oct. 2005.
- [3] J. Devenson, R. Teissier, O. Cathabard, and A. N. Baranov, "InAs/AlSb quantum cascade lasers emitting below $3 \mu\text{m}$," *Appl. Phys. Lett.*, vol. 90, p. xxxxxx, Xxx. 2007.
- [4] M. P. Semtsiv, S. Dressler, and W. T. Masselink, "Short-Wavelength ($\lambda \sim 3.6 \mu\text{m}$) $\text{In}_{0.73}\text{Ga}_{0.27}\text{As}-\text{AlAs}-\text{InP}$ Quantum-Cascade Laser," *IEEE J. Quantum Electron.*, vol. 43, pp. 42–46, Jan. 2007.
- [5] M. P. Semtsiv, S. Dressler, W. T. Masselink, G. Fedorov, and D. Smirnov, "Probing the population inversion in intersubband laser by magnetic field spectroscopy," *Appl. Phys. Lett.*, vol. 89, p. 171105, Oct. 2006.
- [6] M. P. Semtsiv, S. Dressler, W. T. Masselink, "Above room temperature operation of short wavelength ($\lambda = 3.8 \mu\text{m}$) strain-compensated $\text{In}_{0.73}\text{Ga}_{0.27}\text{As}-\text{AlAs}$ quantum-cascade lasers," *Appl. Phys. Lett.*, vol. 85, pp. 1478–1480, Aug. 2004.
- [7] M. P. Semtsiv, M. Wienold, S. Dressler, and W. T. Masselink, "Short-wavelength ($\lambda \sim 3.3 \mu\text{m}$) InP-based strain-compensated quantum-cascade laser," *Appl. Phys. Lett.*, vol. 89, p. 211124, Nov. 2006.
- [8] M. P. Semtsiv, M. Wienold, S. Dressler, and W. T. Masselink, "Short-wavelength ($\lambda \sim 3.05 \mu\text{m}$) InP-based strain-compensated quantum-cascade laser," *Appl. Phys. Lett.*, vol. 90, p. 051111, Jan. 2007.

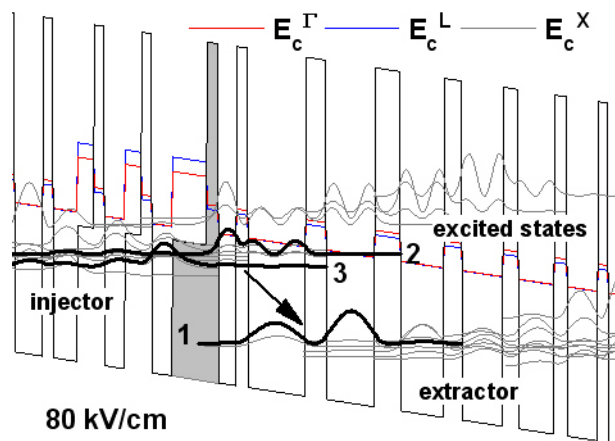


Fig. 1. Conduction band edge energy profile of a single cascade biased for lasing. The probability distributions of the states discussed in text (1, 2, and 3) are drawn with black solid lines. The injector-, extractor-miniband, and excited states are drawn with thin grey lines. Composite injection barrier is highlighted grey colour.

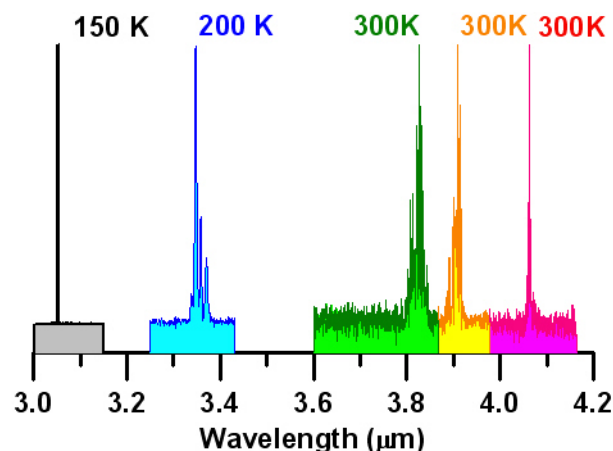


Fig. 2. High-resolution spectra of selected InGaAs-AlAs/InP strain-compensated QCLs with different active-region designs, measured at the indicated temperatures.

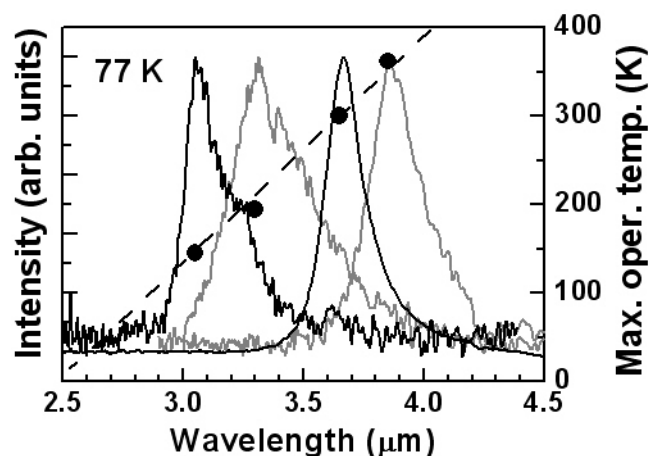


Fig. 3. Low-temperature electroluminescence spectra of four representative QCLs in 2.5–4.5 μm spectral range (solid lines). Full circles are the maximum operation temperatures of the relevant lasers (dashed line is drawn as an eye guide). Full width at the half-maximum of the electroluminescence spectra changes as 32, 40, 17 and 22 meV (from 3 μm to 4 μm) and does not correlate with the maximum lasing temperature.

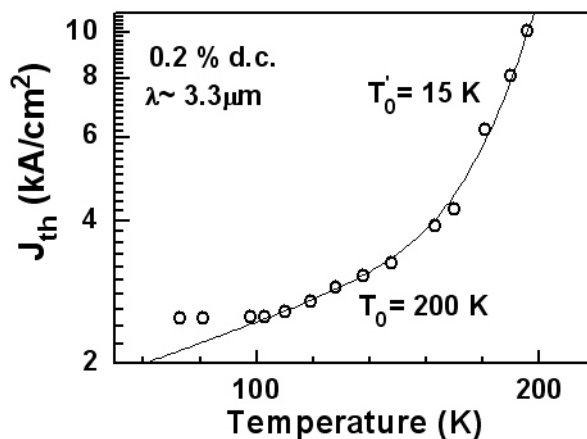


Fig. 4. Threshold current density J_{th} vs. heat sink temperature for a 10 μm wide and 4.5 mm long laser (open circles) driven with 100 ns 20 kHz current pulses. The solid line is a biexponential fit in the 100–200 K temperature range used to determine the two characteristic temperatures T_0 and T_0' .